Image Plane of 3HMS

James G. Hagerman
Hagerman Technology LLC & Pacific Environmental Technologies
September 2005

ABSTRACT

This paper describes the image plane of the new Hyperbolic Helical Horn Mass Spectrometer (3HMS). One of the primary benefits of this device is the capability of parallel spectral readout. That is, a portion of spectrum can be read at any instant, versus the common parameter sweeps over time. The image plane is two-dimensional, with each amu having a specific radial locus. A multi-element detector array can be designed to provide a linear-in-amu spectral readout.

BACKGROUND

The original proposal for 3HMS [1] suggested a two-element detector system, the disc and ring. The center disc acts as a high-pass filter, collecting all ions not rejected by the rotating fields. As the operating parameters are changed, the resonant mass changes with either more or less ions striking the disc. Differentiating the resulting ion current (versus frequency) generates a valid spectrum. The knife-edge of the disc offers maximal resolution. Surrounding the disc is a separate ring detector. It collects only resonant ions, generating a proper spectrum directly.

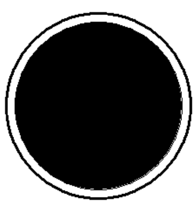

Fig. 1. Disc & ring detector array.

An improved detection scheme capable of exploiting the two-dimensional imagery for parallel readout can be derived by rigorous analysis of the ion trajectory at exit.

ANALYSIS

Figure 2 shows a plot of a resonant ion trajectory through a 3HMS. It is radially symmetric, and the path is that of a corkscrew (helix). As an ion exits the horn it continues on a tangential path. The greater the distance to the detector plane, the greater the magnification of the resonant radius, and the sensitivity to center offset error is reduced.

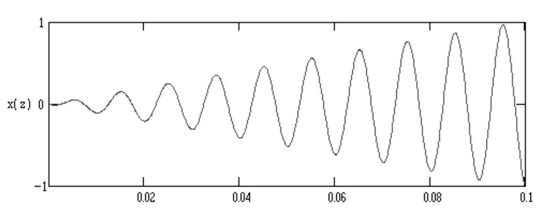

Fig. 2. Ion trajectory, side view.

The rotating electric fields at the exit of the horn assembly are just as critical as at the entrance. The field strength must be decreased as rapidly as possible to prevent further ion deflection. The best way to symmetrically do this is by making the target plane a ground plane, having the same dc potential as the horn grids. This is easy to do since the electrometers used in detection are inherently grounded via feedback. Surrounding the Faraday collectors with a fixed ground completes the target image plane. Figure 3 shows the resulting field using isopotential lines.

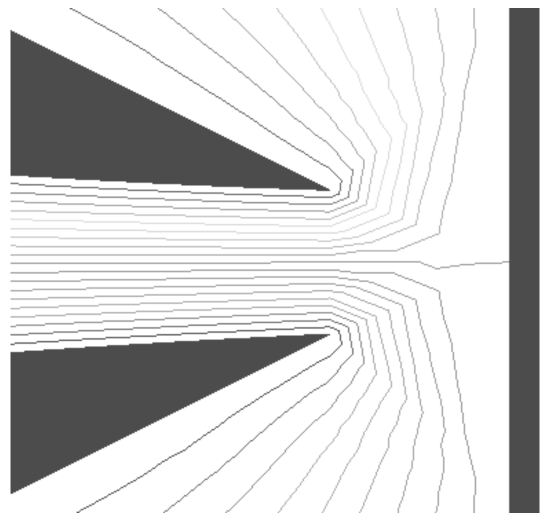

Fig. 3. Electric field between horn exit and image plane.

As it can be seen, the field strength rapidly decreases and changes direction. In fact, it is similar to the field at the horn entrance, but far more abrupt. Therefore, the effect on the ion is smoothly decreased to zero, to where the ion drifts freely. For this analysis, it is assumed that this is close enough to a free field that an ion continues tangentially to the velocity vector given the horn exit. Perhaps the fields can be improved by the addition of another grounded aperture right at the horn exit, or using a cup-shaped shield.

In any case, resonant ions exit the horn at a specific radius. The general formula for this trajectory is given [1] by

$$x(z) \approx -\frac{\mu \cdot q \cdot V}{m \cdot \omega^2} \cdot z \cdot \cos\left(\frac{\omega \cdot z}{v}\right).$$

Figure 4 shows the trajectories of various ion masses for a given set of operating conditions. The light ion crashes into horn grids; heavier ones pass through with decreasing exit angles.

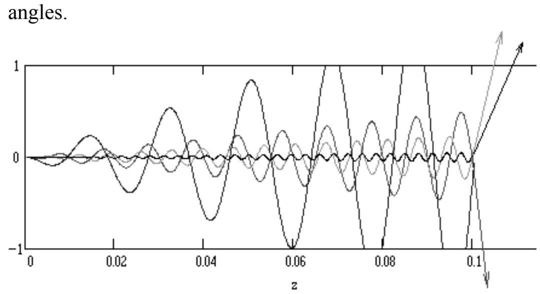

Fig 4. Various ion masses through horn.

Calculating the exit angle is a little difficult, as the ions travel in a helix. That is, there will be some perpendicular axis offset, which effectively increases the resulting target radius. This can be seen looking down the *z*-axis.

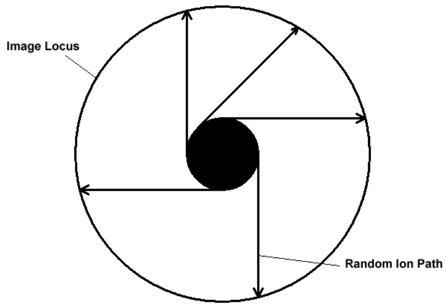

Fig 5. Longitudinal view of ion paths to image plane.

Lengthening the drift distance *d* minimizes the error contributed by the offset, and for now will be ignored. The exit angle is simplified to the case shown in Figure 6.

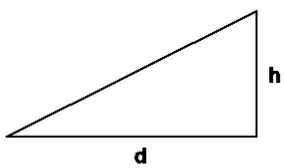

Fig. 6. Exit angle between horn and detector target.

To calculate the exit angle for any given ion mass, we differentiate our previous solution for trajectory.

$$\tan\theta = \frac{h}{d} = \frac{dx(z)}{dz} = \frac{d}{dz}\left[-\frac{\mu \cdot q \cdot V}{m \cdot \omega^2} \cdot z \cdot \cos\left(\frac{\omega \cdot z}{v}\right)\right].$$

This solves as

$$\frac{h}{d} = \left(\frac{\mu \cdot q \cdot V}{m \cdot \omega \cdot v}\right) \cdot z \cdot \sin\left(\frac{\omega \cdot z}{v}\right).$$

Thanks to rotational symmetry, the sine term can be dropped. We then substitute the solution for *v*, and the angle reduces to

$$\frac{h}{d} = \frac{\mu \cdot V \cdot z}{\omega}\sqrt{\frac{q}{2 \cdot m \cdot E}}.$$

The height *h* is the target radius at a given distance *d*. All of the other parameters are known or can be set to desired values. Using the values calculated in the 3HMS paper [1]:

$$z = 0.1$$
$$E = 50$$
$$V = 20$$
$$\mu = 100^2$$
$$m = n \cdot 1.67 \cdot 10^{-27}$$
$$q = 1.6 \cdot 10^{-19}$$
$$\omega = 2 \cdot \pi \cdot f$$

where *n* is the amu count, we arbitrarily set *d* to 5mm (0.005m). The target radial height *h* reduces to

$$h = \frac{15{,}600}{f \cdot \sqrt{n}}.$$

At a frequency of 3.1MHz, we find the ion with $n = 10$ to be resonant. Figure 7 plots the resulting radii at this frequency.

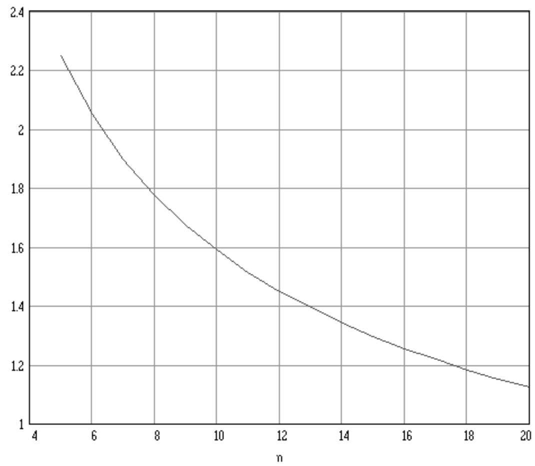

Fig. 7. Target height versus amu, scale in mm.

We now have a general solution for using a plane array detector at any given distance from the horn exit. Ion radius is proportional to the inverse root of *n*. Resolution is reasonable only over a small range, as the heavier ions have an asymptotic solution (zero radius). In the example above, a detector would be practical for parallel spectral readout from about 5 amu to 15 amu.

DETECTOR ARRAY DESIGN

Taking the disc & ring detector concept further, we can place additional rings concentrically, each having a greater radius. This is shown in Figure 8. For a convenient linear-in-amu readout, the radii should have the same square root function as determined above. Such non-linear spacing then results in a perfect parallel spectral readout, using a minimum of detectors.

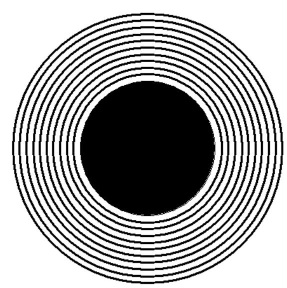

Fig. 8. Multiple ring detector architecture.

CCD TYPE ARRAY

Recent technical advances have made the use of CCD devices practical as ion detectors. Some may be tempted to use a standard two-dimensional CCD type array structure for a detector. This is possible, but does not take advantage of the inherent rotational symmetry of the image plane. A price is paid in complexity, overhead, and efficiency. There is an overwhelming increase in data, proportional to the number of pixels squared. Comparatively, a simple ten-ring detector is the equivalent of a 100 pixel CCD type array. There is a computational penalty for grid decomposition into polar coordinate, summation, and translation of non-linear response to amu. Sensitivity is also partially lost due to charge being spread out over many pixels, instead of just one.

Changing the array structure can alleviate all these problems. Rather that using a rectangular array, one could design a custom CCD using a single readout row in the shape of a spiral, as shown in Figure 9. The radius of such a spiral would be non-linear, following the inverse root function described above. The result would be an extremely fast parallel readout, linear in amu, and having very high spatial resolution.

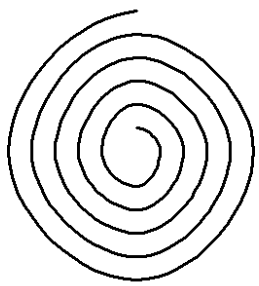

Fig. 9. Spiral shaped CCD topology.

SUMMARY

This paper described the image plane of a 3HMS and appropriate detector array designs. Parallel spectral readout offers speed and throughput benefits for many areas of study. The ability to zoom in on specific peaks quickly and measure just spectral portions is acceptable for applications such as bomb detection or toxic gas monitoring.

REFERENCES

1. “Hyperbolic Horn Helical Mass Spectrometer (3HMS)”, Hagerman, 2005.
2. “Rotating Field Mass and Velocity Analyzer”, Patent 5,726,448, Smith, 1997.